Computer-Aided Design of Selective COX-2 Inhibitors: Comparative Molecular Field Analysis, Comparative Molecular Similarity Indices Analysis, and Docking Studies of Some 1,2-Diarylimidazole Derivatives

G. R. Desiraju,*[,†] B. Gopalakrishnan,*[,‡,§] R. K. R. Jetti,[†] A. Nagaraju,[∥] D. Raveendra,[∥] J. A. R. P. Sarma,*[,⊥] M. E. Sobhia,[‡] and R. Thilagavathi[‡]

School of Chemistry, University of Hyderabad, Hyderabad 500 046, India, Department of Medicinal Chemistry, National Institute of Pharmaceutical Education and Research, Sector-67, S. A. S. Nagar 160 062, India, Molecular Modeling Group, Organic Division-I, Indian Institute of Chemical Technology, Hyderabad 500 007, India, and gvk bioSciences Pvt. Ltd., #210 "My Home Tycoon", 6-3-1192 Begumpet, Hyderabad 500 016, India

Received May 10, 2002

Comparative molecular field analysis and comparative molecular similarity indices analysis were performed on 114 analogues of 1,2-diarylimidazole to optimize their cyclooxygenase-2 (COX-2) selective antiinflammatory activities. These studies produced models with high correlation coefficients and good predictive abilities. Docking studies were also carried out wherein these analogues were docked into the active sites of both COX-1 and COX-2 to analyze the receptor ligand interactions that confer selectivity for COX-2. The most active molecule in the series (**53**) adopts an orientation similar to that of SC-558 (4-[5-(4-bromophenyl)-3-trifluoromethyl-1H-1-pyrozolyl]-1-benzenesulfonamide) inside the COX-2 active site while the least active molecule (**101**) optimizes in a different orientation. In the active site, there are some strong hydrogen-bonding interactions observed between residues His90, Arg513, and Phe518 and the ligands. Additionally, a correlation of the quantitative structure−activity relationship data and the docking results is found to validate each other and suggests the importance of the binding step in overall drug action.

Introduction

Nonsteroidal antiinflammatory drugs (NSAIDs)[1,2] are of immense benefit in the treatment of inflammatory diseases. The principal pharmacological effects of NSAIDs are due to their ability to inhibit prostaglandin (PG) synthesis by blocking cyclooxygenase (COX), which catalyzes the conversion of arachidonic acid to PGH_2.[3] The discovery of two isoforms,[4] COX-1 and COX-2, helped in understanding the side effects associated with NSAIDs. COX-1 is a constitutive enzyme and is necessary for the proper function of the kidney and stomach. In contrast, COX-2 is an inducible isoform that leads to inflammation.[5,6] Classical NSAIDs such as aspirin, ibuprofen, flurbiprofen, and naproxen nonselectively inhibit both forms of COX and also cause gastric and renal failure.[7−10] It is expected therefore that selective inhibition of COX-2 will provide a new generation of NSAIDs with significantly reduced side effects.

There have been sustained efforts concerning the identification of selective COX-2 inhibitors with an attractive pharmacological profile: NS-398, DuP-697, SC-57666, and SC-558 (NS-398, N-(2-cyclohexyloxy-4-nitrophenyl)methanesulfonamide; DuP-697, 5-bromo-2-(4-fluorophenyl)-3-(4-methylsulfonylphenyl)thiophene; SC-57666, 1-[2-(4-fluorophenyl)-1-cylopentenyl]-4-methylsulfonylbenzene; and SC-558, 4-[5-(4-bromophenyl)-3-trifluoromethyl-1H-1-pyrozolyl]-1-benzenesulfonamide), which have been reported as highly selective COX-2 inhibitors.[11−16] Very recently, the COX-2 selective inhibitors celecoxib (Celebrex)[17] and rofecoxib (Vioxx)[18] have been approved by the Federal Drug Administration. These drugs have shown efficacy in the clinical trials of acute pain, osteoarthritis, and rheumatoid arthritis.[19,20] Furthermore, selective COX-2 inhibitors are believed to play a vital role in ovulation and labor as well as in the treatment of colon cancer and Alzheimer's disease.[5,21−23]

Many novel COX-2 inhibitors have been developed by different research groups in the past few years.[24−29] Recently, a novel series of 1,2-diarylimidazoles, which are structurally similar to both celecoxib and rofecoxib that are also selective COX-2 inhibitors, have been reported.[28,29] We too have been analyzing the pharmacophore and the interactions responsible for COX-2 selectivity with three-dimensional quantitative structure−activity relationship (3D QSAR) methods and structure-based docking studies on a series of 1,5-diarylpyrazoles and 3,4-diaryloxazolones.[30,31] In this paper, we report results of analyses using comparative molecular field analysis (CoMFA) and comparative molecular similarity indices analysis (CoMSIA) methodologies, which includes steric, electrostatic, hydrophobic (lipophilic), and hydrogen bond donor and acceptor fields, to derive predictive models from a set of

* To whom correspondence should be addressed. G.R.D.: Tel: 3010 500 ext. 4828. Fax: 91 40 3010 567. E-mail: desiraju@uohyd.ernet.in. B.G.: Tel: 3045 439. Fax: 91 40 3045 438. E-mail: gopalakrishnanb@drreddys.com. J.A.R.P.S.: Tel: 651 9990. Fax: 91 40 6626 885. E-mail: sarma@gvkbio.com.

† University of Hyderabad.

‡ National Institute of Pharmaceutical Education and Research.

§ Present address: Department of Molecular Modeling & Drug Design, Discovery Research, Dr. Reddy's Laboratories Ltd., Bollaram Road, Hyderabad 500 050, India.

∥ Indian Institute of Chemical Technology.

⊥ gvk bioSciences Pvt. Ltd.

10.1021/jm020198t CCC: $22.00
Published on Web 09/20/2002

Scheme 1. Molecules Used for CoMFA, CoMSIA, and Docking Studies

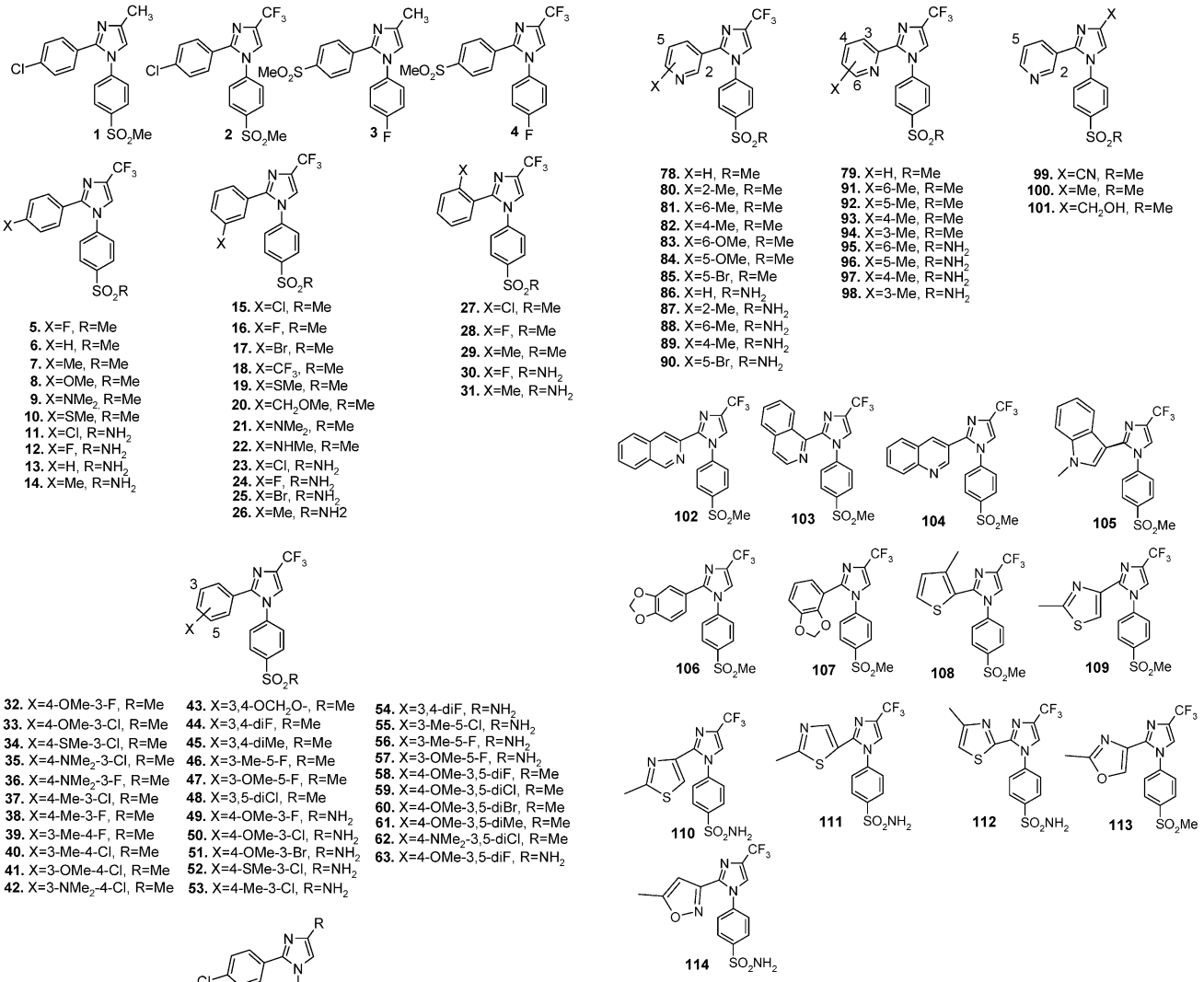

114 analogues of 1,2-diarylimidazoles[28,29] for their COX-2 selectivity. Furthermore, we report docking studies with FlexiDock[32] and Affinity[33] wherein some of the 1,2-diarylimidazole derivatives have been docked into both COX-1 and COX-2.

Computational Details

The chemical structures of the 114 analogues are given in Scheme 1. The biological activities[34] were converted into the corresponding $-\log(IC_{50})$ values. The observed antiinflammatory activities $\{-\log(IC_{50})\}$ for the training and test sets are given in Tables 1 and 2, respectively. The various 3D QSAR studies such as CoMFA and CoMSIA were carried out using SYBYL,[32,35] while the docking studies were carried out using FlexiDock and Affinity in SYBYL and InsightII[33] environments, respectively.

Molecular 3D Structure Building. All molecules were generated based on the coordinates of the molecule SC-558 (6COX).[36,37] All structures were minimized using Tripos force fields and the conjugate gradient algorithm with a gradient convergence value of 0.01 kcal/mol Å. Partial atomic charges were calculated using the Gasteiger−Hückel method. Initially, a constrained minimization for 100 cycles was performed in which the three rings A, B, and C (Frame 1) were defined as an aggregate to constrain their conformation and to avoid false minima. The constraints were then removed, and the structure was subjected to 1000 cycles of minimization or till the gradient converged to 0.001 kcal/mol Å. Further geometric optimizations were performed using AM1 methods in order to get accurate molecular structures and electrostatic potential (ESP) charges. Default parameters in MOPAC were used for structural optimization. These optimized structures and charges were used in the CoMSIA and CoMFA studies. The final geometry of these molecules is very similar to that of SC-558 inside the COX-2 enzyme.[36,37]

Alignment. The most active compound **53** was used as the template, and the rest of the molecules were

Table 1. Experimental −log(IC_{50}) and Corresponding Model Predicted Values of Molecules Used in the Training Sets for CoMFA and CoMSIA

		predicted				predicted	
compd	actual −log(IC_{50})	CoMFA 2	CoMSIA (S, E, H, A)	compd	actual −log(IC_{50})	CoMFA 2	CoMSIA (S, E, H, A)
1	0.62	0.10	0.19	**58**	0.77	1.15	0.60
3	−2.00	−1.98	−1.71	**59**	0.85	0.93	0.89
5	1.00	0.97	1.04	**61**	0.14	0.19	0.30
6	0.92	0.56	0.62	**62**	0.85	0.99	1.03
7	0.80	0.82	0.80	**63**	1.52	1.98	1.23
8	0.24	−0.07	0.04	**64**	0.21	−0.06	0.32
9	0.15	0.38	0.62	**66**	−0.20	−0.20	−0.62
10	0.80	0.58	0.88	**67**	0.64	1.07	0.42
11	2.00	1.85	1.90	**69**	−2.00	−2.10	−2.07
13	1.40	1.26	1.28	**70**	0.62	0.93	0.84
14	1.40	1.57	1.45	**71**	1.52	1.66	1.41
15	1.22	0.93	1.09	**72**	1.30	1.18	1.44
16	0.92	0.80	0.84	**74**	−0.92	−0.93	−0.98
17	1.10	0.88	1.27	**75**	0.49	0.53	0.41
18	0.68	0.70	1.09	**76**	−2.00	−1.84	−2.11
19	0.46	0.19	0.34	**78**	−0.23	−0.21	−0.48
20	−1.83	−1.43	−1.99	**79**	−0.18	−0.27	−0.39
23	2.10	1.75	1.77	**80**	−0.98	−0.96	−1.45
24	1.52	1.32	1.50	**82**	−1.73	−2.14	−1.76
25	2.15	1.71	1.95	**83**	−0.08	0.22	−0.08
26	1.52	1.21	1.27	**85**	0.02	−0.52	−0.23
27	0.05	−0.14	0.37	**86**	0.36	0.58	0.22
28	0.40	0.00	0.42	**87**	−0.45	−0.14	−0.79
30	1.00	0.82	1.07	**88**	0.54	0.87	0.69
31	0.70	0.76	0.83	**89**	−1.71	−1.36	−1.10
32	0.82	1.00	0.57	**90**	0.47	0.25	0.44
34	1.40	1.12	1.34	**91**	−0.46	−0.58	−0.25
36	0.48	0.64	0.72	**92**	−0.11	−0.10	−0.28
37	1.52	1.34	1.28	**94**	−0.76	−0.66	−0.56
38	0.96	1.22	1.03	**95**	0.38	0.10	0.39
39	0.77	1.17	1.02	**96**	0.14	0.61	0.36
40	1.05	1.32	1.23	**97**	0.36	0.32	0.29
41	0.60	0.98	0.93	**98**	−0.19	0.07	0.09
43	0.77	0.37	0.40	**100**	−1.90	−1.56	−1.55
45	0.42	0.85	0.78	**101**	−2.97	−2.61	−2.71
47	0.02	0.19	−0.21	**102**	−0.08	−0.28	−0.03
48	0.77	0.68	1.20	**104**	0.20	−0.30	0.08
50	1.70	1.77	1.59	**105**	−0.04	−0.17	−0.21
51	1.52	1.81	1.72	**106**	0.55	0.49	0.44
52	2.00	1.85	2.00	**109**	0.03	−0.30	−0.18
53	2.52	2.14	1.96	**110**	0.28	0.38	0.45
54	1.52	1.60	1.96	**111**	0.37	0.67	0.66
55	1.40	0.97	1.36	**112**	0.96	0.58	0.87
56	1.52	1.41	1.30	**113**	−0.62	−0.13	−0.12
57	0.34	1.05	0.46	**114**	0.39	0.31	0.29

aligned to it by using fragment 1 as the substructure as described earlier.[31] Molecular alignment has also been carried out with field fit methods using SYBYL.[32]

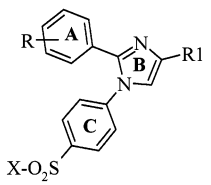

Frame 1

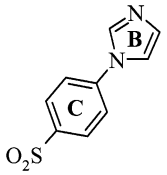

Fragment 1

CoMFA. CoMFA fields were generated using standard procedures.[35] The coordinates of the CoMFA grid box are (−10.87, −11.03, −9.77) and (13.10, 10.96, 7.62) for the lower and upper corners, respectively. The total number of the grid points generated is 1296. It is essential to assess the predictive power of the CoMFA model by using a set of compounds that are referred to as the test set. Therefore, the total set of inhibitors initially considered is divided into two groups in the approximate ratio 4:1 (90 in the training set to 24 in the test set). The selection of test set and training set compounds was done manually such that low, moderate, and high activity (IC_{50}) compounds occur in roughly equal proportions in both sets.

CoMSIA. The same grid constructed for the CoMFA field calculation was used for the CoMSIA field calculation.[35] The CoMSIA method avoids some inherent deficiencies of the Lennard−Jones and Coulomb potentials used in CoMFA to calculate the field energies around a set of aligned ligands. In CoMSIA, a distance-dependent Gaussian type functional form has been employed that avoids singularities at the atomic positions and dramatic changes of potential energy for those grid points in the proximity of the surface; no arbitrary definition of cutoff limits is required in CoMSIA. A probe atom sp^3 carbon with charge +1, hydrophobicity +1, and H-bond donor and acceptor property as +1 was placed at every grid point to measure the electrostatic, steric, hydrophobic, and H-bond donor or acceptor field. The value of the attenuation factor was defined as 0.3. Finally, the results from field calculations combined with the observed biological activities were included in

Table 2. Actual COX-2 Inhibitory Activity $-\log(IC_{50})$, the Predicted Activities from Different CoMFA and CoMSIA Models, and the Residual Values for Test Set Molecules

		predicted	
compd	actual (IC_{50})	CoMFA 2	CoMSIA (S, E, H, A)
2	0.96	1.13	1.26
4	−0.77	−0.74	−2.31
12	2.00	1.74	1.69
21	−0.51	−0.74	−0.05
22	0.04	0.05	−0.20
29	0.10	−0.07	0.18
33	0.89	1.05	0.82
35	0.49	0.71	0.94
42	−0.02	0.12	0.82
44	0.92	0.94	1.31
46	0.96	0.96	0.64
49	1.52	1.68	1.29
60	1.05	1.46	1.32
65	0.39	0.21	0.02
68	−0.76	0.09	−0.89
73	−0.57	0.01	−0.88
77	−0.19	−0.88	0.00
81	−0.26	0.12	−0.02
84	−1.57	−0.31	−0.74
93	0.28	−0.39	−0.35
99	−1.39	−0.32	−1.32
103	−0.23	−0.54	−0.47
107	0.33	−0.32	0.01
108	−0.04	−0.93	0.27

a molecular spreadsheet and partial least squares (PLS) methods were applied to generate the CoMSIA model. To choose the appropriate components and check the statistical significance of the models, the PLS algorithm with the leave-one-out cross-validation method was employed. The CoMSIA results were graphically interpreted by field contribution maps using the field type "STDEV*COEFF".

Structure-Based Studies. Docking studies were carried out using FlexiDock[32] and Affinity[33] for 1,2-diarylimidazole molecules in both forms of COX. The crystal structures of murine apo-COX-2 (6COX) with SC-558[36,37] and sheep COX-1 (1PGG) with iodoindomethacin (IMM)[38] (IMM, indomethacin 1-(4-choroben-zoyl)-5-methoxy-2-methyl-1H-indole-3-acetic acid) were used in this study. Such a procedure is valid because the extent of structural differences in the active site between COX-1 (or COX-2) from different species was negligible as compared to differences between COX-1 and COX-2 themselves in the active site. Hydrogens were added to the proteins while all of the residues were considered in the neutral form. Active sites of COX-1 and COX-2 were defined using the inhibitors IMM and SC-558, respectively, and all amino acid residues within a 5.0 Å radius to any of the inhibitor atoms were considered. All ligands were positioned in an orientation similar to that of IMM or SC-558 prior to docking.

FlexiDock. All ligand molecules (**1**−**114**) that were included for 3D QSAR studies were used in the FlexiDock docking study. The backbone conformation of residues in the binding pockets of the enzymes was kept rigid, while all rotatable bonds of the ligands were kept flexible to explore the most biologically active conformation. Docking studies were performed for 10 000 generations, and only the energetically favorable complexes/conformations were analyzed. On the basis of the fitness score (energy), one complex structure for each ligand was selected as the best fit and its score was correlated with its biological activity.

Affinity. Affinity studies are carried out only for representative molecules—the most active molecule **53**, a moderately active molecule **59**, and the least active molecule **101**. These are docked into the active site of COX-2 and COX-1 enzymes as described earlier.[31] All of the residues in the active site were also allowed to move freely along with internal bonds of the ligand.

Results and Discussion

The models generated by CoMFA and COMSIA methods are summarized in Table 3. They were analyzed for their predictive ability for the training set as well as test set molecules. Final models were selected primarily based on the values of better cross-validated r^2, predictive r^2, and the SD values of test set molecules (all of these values are highlighted in Table 3).

CoMFA Analysis. Two CoMFA models, CoMFA 1 (database alignment) and CoMFA 2 (field fit alignment), were considered in the final analysis (Table 3). In these two models, the cross-validated r^2 values are 0.568 and 0.488, respectively, with six components and noncross-validated r^2 values are around 0.93 with standard error of estimation values (SEEs) of 0.281 and 0.292, respectively. Both models are equally good, even for the test set molecules; in general, their performance can be termed as moderate. In these two CoMFA models, the steric and electrostatic field contributions are 55:45 indicating a nearly equal influence of these two fields on ligand−receptor interactions. Both of the models demonstrated a good predictive ability.

The CoMFA analysis gives contour plots of steric and electrostatic interactions. The steric interactions are represented by green- and yellow-colored contours (Figure 1). Bulky substituents in the regions shaded yellow are likely to decrease biological activity, while bulky group substitution in the green-colored regions is likely to enhance the activity. Green-colored regions near the para and meta positions of ring A show that medium-sized substituents increase biological activity because of their positioning near the end of the active site cleft that extends toward the peroxide catalytic site. Blue- and red-colored contours (Figure 1) represent CoMFA electrostatic fields. The groups with positive ESP in the blue areas (between one of the meta positions and the para position in ring A) increase activity. Electronegative groups in the red-colored region (4-position of ring B) enhance the biological activity of the molecule. It may be observed in general that the structural variations are predominantly on ring A and to some extent on ring B.

The predicted activities from the CoMFA models for the molecules with substituents on ring A at the meta position, **15**−**18** and **23**−**26**, and substituents at meta or para positions, **32**−**63**, are in reasonable agreement with the actual activities (Table 1). Only a few molecules (**27**−**31**) are ortho-substituted on ring A, and they are also less active. Substitution at this position probably influences the conformation of ring A. This ortho effect was observed previously for the 3,4-diaryloxazolones.[31]

Molecules with substituents other than $-CF_3$ at the 4-position of ring B, namely, **64**−**77** and **99**−**101**, are less active whereas **67** and **70**−**72** are moderately active (Table 1). However, molecules **68**, **77**, and **99** with

Table 3. Results of CoMFA and CoMSIA Studies on COX-2 Selective Inhibitors

		CoMSIA				
fields	CoMFA	S, E, H, D, A	S, E	S, E, H	S, E, H, A	S, E, H, D
			Database Alignment[a]			
r^2 [c]	**0.568**	**0.774**	0.490	0.758	**0.775**	0.753
SEP[d]	0.707	0.515	0.768	0.533	0.510	
no. components[e]	6	7	6	7	6	7
r^2 [f]	0.932	0.950	0.881	0.947	0.946	0.942
SEE[g]	0.281	0.243	0.372	0.249	0.249	0.260
F value[h]	189.079	220.753	102.088	210.237	244.067	190.875
field contributions[i]	0.55, 0.46	0.12, 0.31, 0.30, 0.10, 0.17	0.23, 0.77	0.15, 0.42, 0.43	0.12, 0.33, 0.36, 0.18	0.14, 0.39, 0.35, 0.12
$r^2_{\text{test set}}$	**0.794**	**0.820**	0.654	0.765	**0.855**	0.759
$SD_{\text{test set}}$	**0.530**	**0.490**	0.630	0.594	**0.501**	0.583
			Field Fit Alignment [a]			
r^2 [c]	**0.488**	0.772	0.488	0.754	0.774	0.752
SEP[d]	0.770	0.517	0.770	0.536	0.511	0.539
no. components[e]	6	7	6	7	6	7
r^2 [f]	0.927	0.950	0.882	0.948	0.947	0.943
SEE[g]	0.292	0.241	0.369	0.247	0.248	0.259
F value[h]	174.410	224.428	103.77	213.875	247.175	193.619
field contributions[i]	0.554, 0.446	0.12, 0.31, 0.30, 0.10, 0.17	0.23, 0.77	0.15, 0.42, 0.43	0.12, 0.33, 0.36, 0.18	0.14, 0.39, 0.36, 0.12
$r^2_{\text{test set}}$	**0.800**	0.811	0.652	0.760	0.840	0.760
$SD_{\text{test set}}$	**0.498**	0.485	0.628	0.591	0.490	0.585

[a] Two alignment methods were employed in the generation of CoMFA and CoMSIA models. [b] CoMFA and CoMSIA with different field combinations such as steric (S), electrostatic (E), hydrophobic (H), donor (D), and acceptor (A) fields. [c] Cross-validated correlation coefficient. [d] Standard error of predictions. [e] Optimum number of components obtained from cross-validated PLS analysis and same used in final noncross-validated analysis. [f] Noncross-validated correlation coefficient. [g] Standard error of estimate. [h] F-test value and Prob of $R^2 = 0$ ($n1 = 6$, $n2 = 17$). [i] Field contributions: steric and electrostatic fields from CoMFA. Steric, electrostatic, hydrophobic, donor, and acceptor fields from CoMSIA.

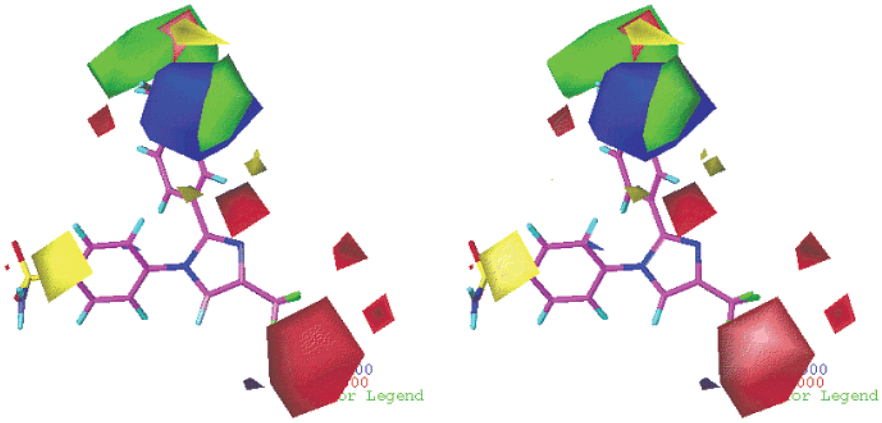

Figure 1. Stereoview of CoMFA steric and electrostatic contour plots (STDEV*COEFF) from CoMFA 2. Molecule **53** is displayed in the background for reference.

$-COOCH_2CH_3$, $-CH_2CN$, and $-CN$ substituents at the 4-position of ring A are less active. The calculated activities of these molecules from both models are similar to the experimental values. From the CoMFA analysis alone, it is difficult to analyze the effect of substituents such as $-SO_2CH_3$ and $-SO_2NH_2$ groups at the para position of the ring C. However, these substituents are found to exert changes in binding energies as will be discussed later in the docking studies.

CoMFA electrostatic contour plots (Figure 1) suggest that electronegative substituents at the 4-position of ring B could increase the biological activity. While the $-CF_3$ group enhances the activity, others such as $-CN$ and $-CH_2CN$ groups are ineffective; these molecules are less active and are so predicted by the CoMFA models. One of the reasons for this could be that the highly accumulated electron density at this position in these molecules may cause unfavorable electrostatic interactions with the receptor atoms.

Molecules **107** and **108** have substituents at the ortho position on ring A; molecule **107** is moderately active while molecule **108** is less active. The small yellow region at the ortho position of ring A in the CoMFA steric contour plot (Figure 1) indicates that any bulky group substitution at this position would decrease the activity of the molecule; both CoMFA models predicted them to be less active molecules albeit with large residual values. Molecule **84** is also a less active molecule, and both models predicted it as such. Thus, the predictive ability of these models is very good; between these two CoMFA models, CoMFA 2 with high predictive $r^2_{\text{test set}}$ (0.80) and a low $SD_{\text{test set}}$ (0.498) has better predictive ability over the CoMFA 1 model. The actual vs predicted activities graphs were plotted in Figure 2 for CoMFA 2 model wherein most of the

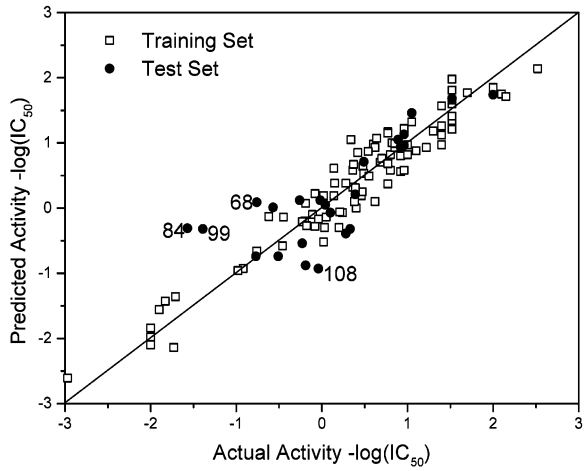

Figure 2. Actual vs predicted activity for the model CoMFA 2. The molecules that deviate from the diagonal are labeled.

molecules are on or near the diagonal line, which indicates good predictive ability.

CoMSIA Analysis. Various CoMSIA models were generated employing two alignment methods and with different field combinations. Two models were found to be better based on the values of their cross-validated r^2 and predictive r^2 of test set molecules. There is no significant difference observed between the CoMSIA models developed by database and field fit alignment methods. Therefore, the models that were generated by database alignment with slightly higher cross-validated r^2 were considered for the final analysis.

The PLS analysis of the CoMSIA model that was generated using only steric and electrostatic fields produced a cross-validated r^2 of 0.490 with an optimum number of six components and the corresponding non-cross-validated r^2 as 0.881 with a SEE value of 0.372. The PLS analysis of the CoMSIA model that was generated by employing all five fields produced a cross-validated r^2 of 0.774 with seven components and the noncross-validated r^2 value of 0.950 with 0.243 as the SEE (Table 3). The high r^2 values of this CoMSIA model indicate the importance of contributions from other fields (lipophilic, donor, and acceptor) to the biological activity.

The CoMSIA steric and electrostatic fields based on PLS analyses are represented as 3D contour plots in Figure 3a. The steric interactions are represented by green- and yellow-colored contours while the electrostatic fields are represented by blue and red contours. The green-colored contours around the rings A and B suggest that the introduction of steric groups in these regions will induce sterically favorable interactions between ligand and receptor.

The situation with respect to ring B is more important and interesting. The blue-colored contour on the ring itself accompanied by a red-colored contour at the 4-position of the ring indicates that an electron-withdrawing group at this position may be ideal (Figure 3a). Such a substituent would not only make the ring electron deficient but also lead to an accumulation of charge at or near the 4-position. Further examination of the lipophilic and steric fields indicates that bulkiness of this (electronegative) substituent is also preferred (Figure 3a−c). Substituent groups that combine both electronegativity and lipophilicity such as $-CF_3$, $-CHF_2$, $-CH_2F$, $-CN$, $-C_6H_5$, $-CH_2O$-C_6H_4-(4-Cl), and $-CH_2S$-C_6H_4-(4-Cl) may be best-suited for activity.

The CoMSIA hydrophobic contour plots are represented in Figure 3b. Molecules with small polar substituents on ring A at the para and meta positions (**2**, **5**, **11**, **12**, **16**−**18**, **23**−**25**, and **32**−**63**) are moderately active. The CoMSIA donor and acceptor contour plots are shown in Figure 3c. The cyan contour observed on the NH_2 group of ring C indicates that hydrogen bond donor substituents at this position enhance the inhibitory activity by forming hydrogen bonds with various amino acid residues of the receptor. The molecules with $-SO_2NH_2$ substitution rather than $-SO_2CH_3$ at this position are more active. The purple-colored contours observed near the SO_2 group of ring C and the 4,5-positions of ring A indicate that substitution of the hydrogen bond donor groups at this position may decrease the activity of molecule. Thus, molecule **4**, which has no SO_2 substituent at this position, is less active.

The last CoMSIA model with steric, electrostatic, hydrogen-bonding, and hydrophobic fields predicted the biological activities of the majority of the test set molecules with reasonable accuracy resulting in low residual values (Table 2 and Figure 4a). However, like other models, it also failed to predict activities of three molecules, namely, **4**, **42**, and **84**. These three molecules are identified in Figure 4a and can be treated as outliers. However, the CoMSIA models demonstrated somewhat better predictive abilities than the simple CoMFA models and these studies can be used routinely to design new compounds for selective inhibition of COX-2.

CoMFA vs CoMSIA. A comparison of the models derived from CoMFA and CoMSIA was made to assess their relative predictive abilities, especially for the outliers. Satisfyingly, all of the outliers are for the least active compounds such as **4**, **84**, and **108**. This suggests that the differences between CoMSIA and CoMFA are not glaring. The switching of A and C rings in **4** may be the reason CoMSIA could not predict this molecule well while CoMFA predicts it correctly. CoMFA predicted the activity of molecule **42** exactly whereas in CoMSIA, the residual values are quite high (−0.83 and 0.84). The probable reason is that CoMSIA scales steric fields less strongly than CoMFA. An interesting observation is that CoMSIA predicts **108** better than CoMFA. The reason for this could be the hydrophobic character of the thiophene ring. In summary, it can be said that both of the models have limitations. While some molecules are outliers (residuals more than 1.0) for CoMFA (**68**, **99**, and **108** in Figure 2) or CoMSIA (**4** and **42** in Figure 4a), molecule **84** is an outlier in both approaches hinting that a remeasurement of its activity may be useful.

Figure 4b compares the predicted activities of both models relative to one another for the training and test set molecules. It was observed that while high and moderately active molecules are predicted with equal ease in both models, less active molecules differ in both models. Nearly equal strengths of steric and electrostatic fields in both models (0.55 and 0.46, respectively, in CoMFA and 0.48 (S + H) and 0.53 (E + A), respectively, in CoMSIA) suggest only minor differences

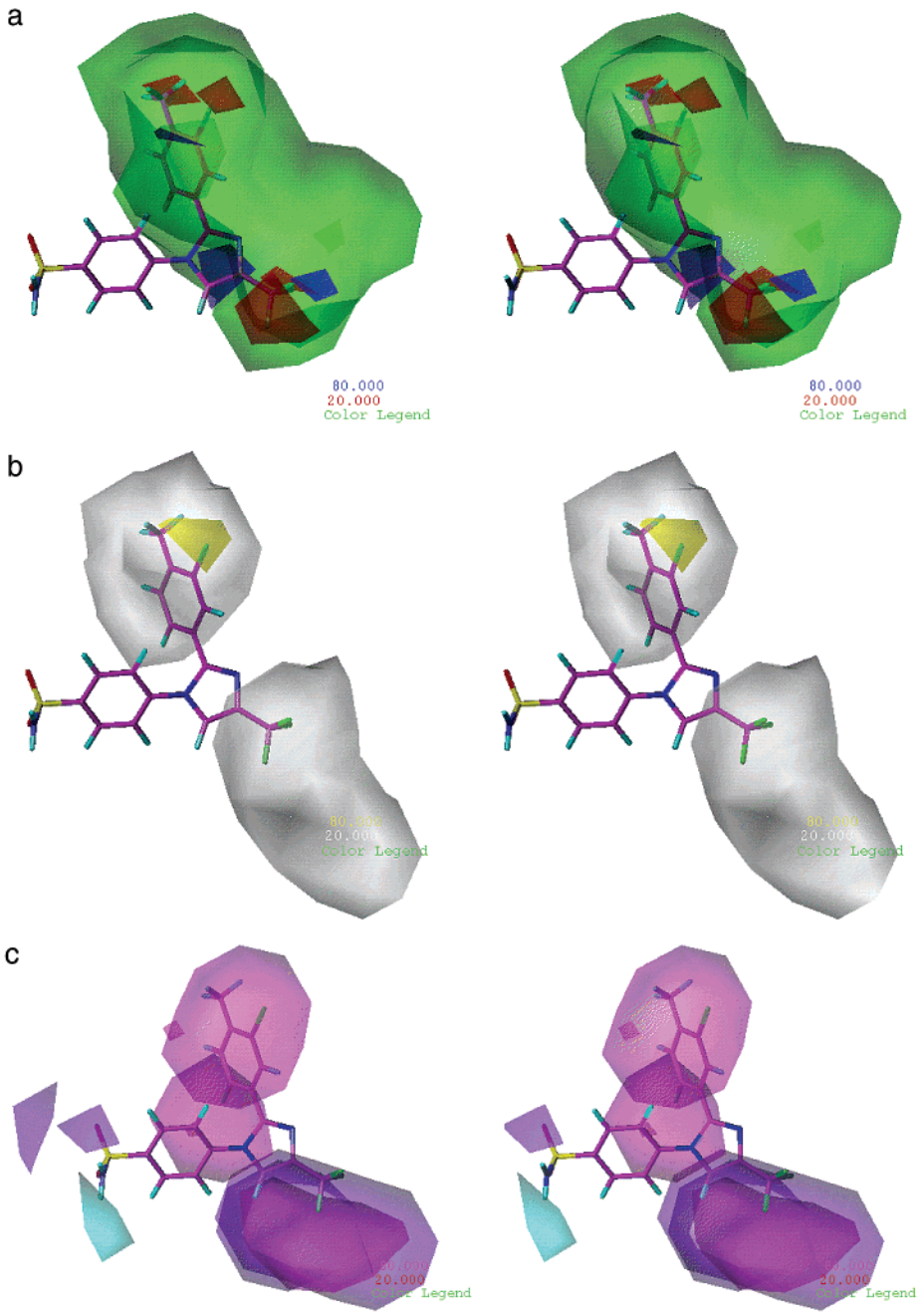

Figure 3. Stereoview of the contour plots of the CoMSIA (a) steric and electrostatic fields, (b) hydrophobic fields, and (c) hydrogen bond donor and acceptor fields. The most active molecule **53** is displayed for reference.

between them. While the lipophilic character of the B ring is predominant in the CoMFA model, meta substitution for ring A is strongly indicated in CoMSIA.

Docking Studies. FlexiDock. All of the 114 ligands have been docked into both COX-1 and COX-2 using genetic algorithm techniques using FlexiDock, and the docking scores for the best possible conformation and orientation have been correlated with its observed biological activity (Figure 5a). Docking results of all diarylimidazoles with COX-2 show better correlation with biological activity; molecules with higher activity exhibited better docking scores (lower energies). However, docking of various imidazoles into the COX-1 active site showed a variable correlation between the observed inhibitory activities and the fitness scores. Barring a few false positives, almost all of the ligand molecules bind with less favorable scores (positive/repulsive energies) when compared to the corresponding COX-2 complexes. Validity of these calculations is established from the absence of false negatives, in other words the absence of molecules that bind poorly and yet show high activity. These observations concur with the fact that all of these molecules are relatively weak inhibitors of COX-1. The orientations of most of the imidazoles in COX-2 are similar to that of SC-558,[35] whereas they assume orientations that are different from that of IMM in COX-1.[38]

Another facet of our calculations is the prediction of selectivity. In Figure 5b, the observed and predicted selectivities are shown with respect to the COX-2 activity. While the observed selectivity is measured from the ratio of IC_{50} values, the predicted selectivity is given

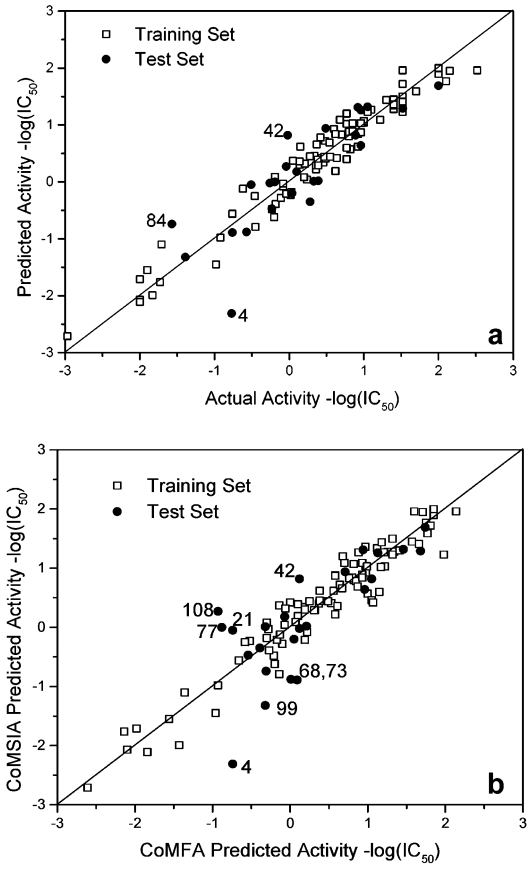

Figure 4. (a) Actual vs predicted activity for the model CoMSIA 2. (b) Predicted activity of the CoMFA and CoMSIA models. The molecules that deviate the most from the diagonal (outliers) are labeled.

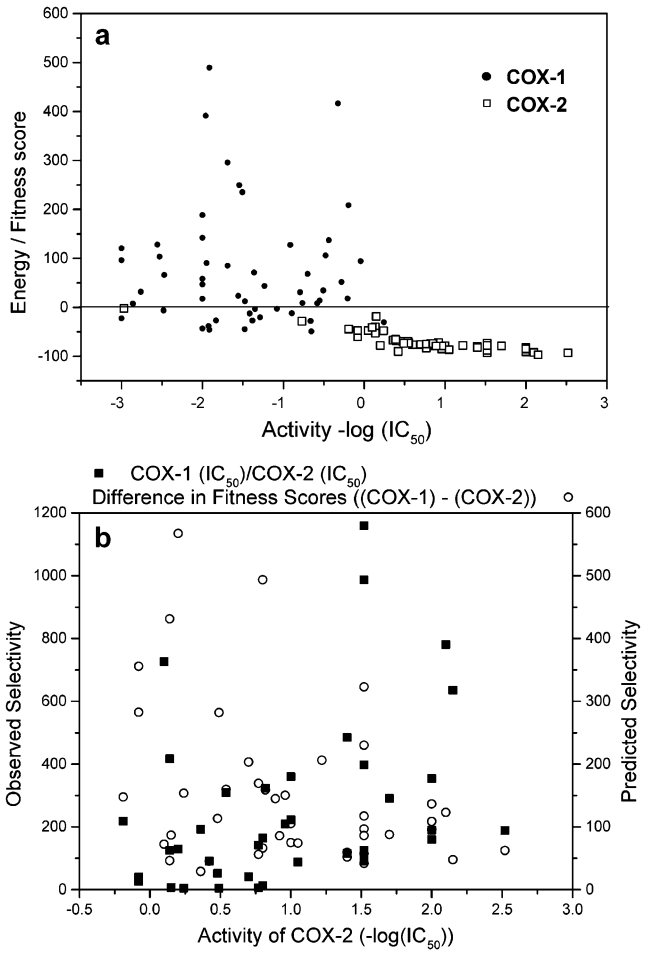

Figure 5. (a) Fitness scores vs biological activities of diarylimidazoles **1**−**114**. The observed biological activities of all ligands with COX-1 and COX-2 are considered as $-\log(IC_{50})$ and are given on the abscissa while the ordinates represent the corresponding scores. While most of the molecules indicate very low fitness scores with respect to COX-2 indicating very good binding, they have very high scores with respect to COX-1 indicating very low affinity to bind in the active site. (b) Observed and predicted selectivities of COX-2 over COX-1 are plotted with respect to COX-2 activities. While the observed selectivity increases from low to high COX-2 active molecules, the predicted selectivity follows an opposite trend.

as the difference in the fitness scores. While there is a general positive trend, in that most of the molecules that are predicted to have higher COX-2 selectivity do have observed selectivity, the trend differs as a function of COX-2 activity. Molecules with high COX-2 activity (pIC_{50} values) possess higher selectivity than predicted, while molecules with low COX-2 activities and lacking in selectivity are predicted to have slightly higher selectivities. The reasons for such variation are not apparent but could arise from solvation effects and the flexibility of active site amino acid residues. To address such issues, affinity calculations have been undertaken wherein the amino acid residues in the active site were also varied during the docking process and where solvation effects were implicitly included.

Affinity. Docking of each of the three representative ligands (**53**, **59**, and **101**) into the COX-2 active site generated a number of possible structures with different orientations (and energies) of ligand inside the active site. The most energetically favorable conformation for each ligand in the COX-2 complex was chosen for further analysis. The orientation and hydrogen-bonding interactions of ligand **53** within the COX-2 active site are shown in Figure 6a. The orientation is similar to that of SC-558 (6COX).[35] Different sets of hydrogen-bonding interactions with residues His90 (N−H···O═S 1.95 Å; all distances are for d_{H-X}), Gln192 (C═O···H−N 2.14 Å), Leu352 (C═O···H−N 1.69 Å), and Phe518 (N−H···O═S 2.69 Å) are observed. Molecule **53** showed favorable van der Waals and electrostatic interactions with His90, Val349, Leu352, Ser353, Tyr355, and Val523 (important for selectivity). It also showed some interactions with Tyr348, Arg513, Ala516, Phe518, Met522, and Ser530.

The number of observed hydrogen-bonding interactions between the sulfonamide moiety and the various amino acid residues at the entrance of the COX-2 active site enables the molecule **53** to be a strongly binding and selective COX-2 inhibitor.[38,39] The substituents (4-CH_3 and 3-Cl) on the ring A also induce favorable electrostatic interactions between various amino acid residues at the bottom of the active site (hydrophobic cleft) and ring A (Figure 6a).

The orientation of the moderately active molecule **59** is similar to that of the highly active molecule **53**. Hydrogen-bonding interactions of **59** with His90 (N−H···O═S 2.51 Å), Arg513 (N−H···O═S 2.15 Å), and Phe518 (N−H···O═S 2.97 Å) are observed. These interactions are relatively weak as compared to those formed by molecule **53**. The replacement of the $-SO_2-$

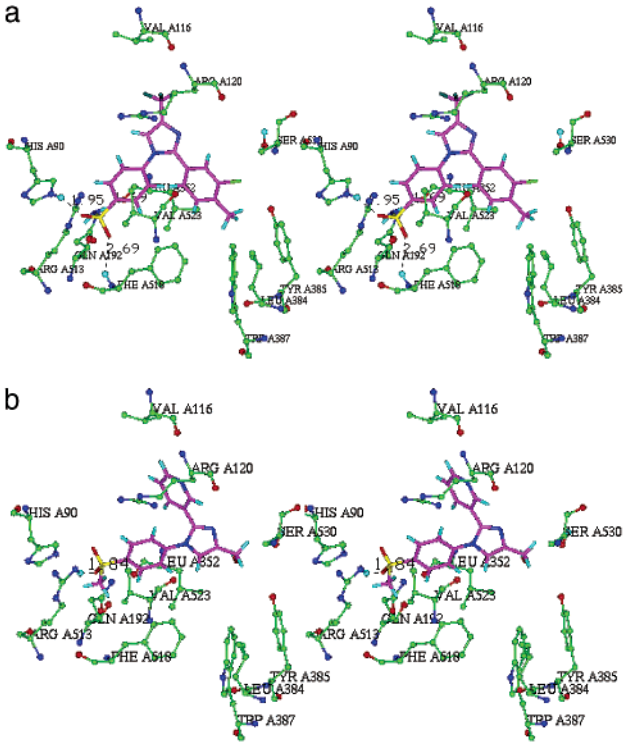

Figure 6. (a) Stereoview of the molecule **53**−COX-2 complex; the figure was generated by Affinity. The hydrogen-bonding interactions are shown as broken lines. The ligand is shown in magenta. All protein hydrogens are removed for clarity. (b) Stereoview of the molecule **101**−COX-2 complex. The hydrogen-bonding interactions are shown as broken lines. The ligand is shown in magenta. Notice the difference in the orientation of ligand in the active site when compared with panel a.

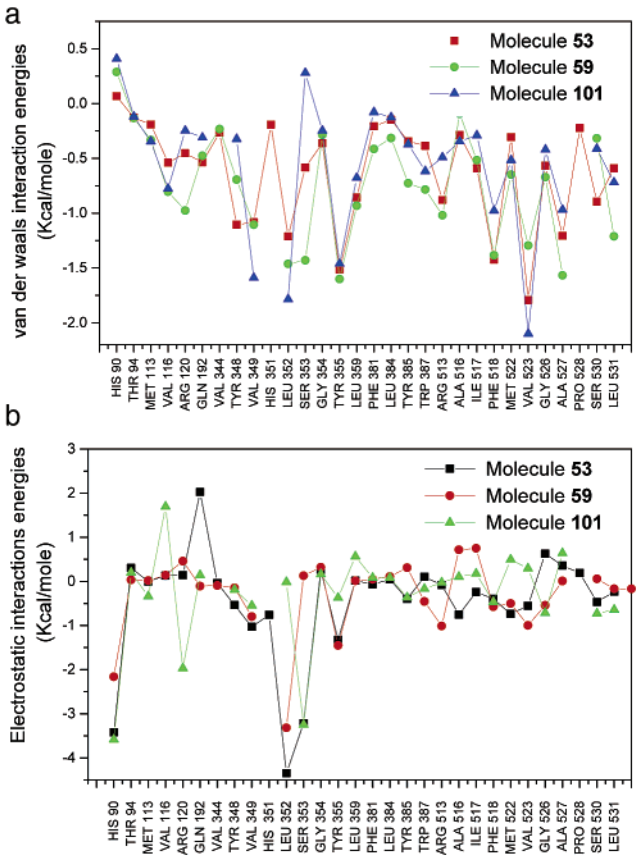

Figure 7. Steric (a) and electrostatic (b) contributions to the nonbonded interaction energies between molecules **53**, **59**, and **101** with various residues of the active site of COX-2.

NH_2 group in molecule **53** with the $-SO_2CH_3$ group in molecule **59** is the main reason for these weaker interactions and hence lower activity. Substituent effects such as these have been reported recently.[39]

Molecule **101**, which is a less active COX-2 inhibitor, is bound in a totally different orientation from that of molecule **53** and SC-558 at the COX-2 active site and is shown in Figure 6b. The observed orientation is unique and is not observed with any other class of ligand that was docked into the COX-2 active site. The $-CH_2$-OH-substituted ring B ($-CF_3$ in almost all active molecules including the highly active molecule **53**) of the molecule **101** moved toward the hydrophobic cleft of the active site. As a result, ring A, which is replaced by a heterocyclic ring (pyridine) in molecule **101**, occupies the position of ring B in COX-2−SC-558 or COX-2−molecule **53** complex. Such an orientational preference may be due to strong electrostatic interaction between the Arg120 and the pyridyl moiety of ring A (Figure 7b). In addition, a hydrogen bond between the Arg513 (N−H···O═S 1.84 Å) and the sulfonyl group of ring C was observed. This also resulted in some favorable interactions throughout the active site with residues such as His90, Arg120, Val349, Ser353, and Val523 (Figure 7a,b). Interactions with various residues at the entrance of the active site, Val116, Phe381, and Met522, are less favorable, and interactions with other residues, Val344 and His351, are very weak.

The steric interaction energies of diarylimidazoles **53**, **59**, and **101** with various amino acid residues in the active site are plotted in Figure 7a while the electrostatic contributions are given in Figure 7b. In general, molecules **53** and **59** show similar types of interactions with various amino acid residues in the active site. Molecule **101** is involved in a different pattern of interactions throughout the COX-2 active site, as might be expected. The electrostatic interactions of molecule **101** deviated greatly from those of molecules **53** and **59**. This difference may contribute to the lower activity of molecule **101**. In the case of molecules **53** and **101**, the preferred orientations indicate that while the position of ring C is conserved, the positions of ring A and ring B are interchanged. This is easier to understand because the electronegative $-CF_3$ group in **53** has been replaced with an electropositive $-CH_2OH$ group. Because this electronegative group interacts strongly with Arg120, the change in functional group results in an orientational change bringing the pyridine nitrogen of ring A in **101** close to Arg120. Nonbonded interaction energies between ligand and all amino acid residues in the active site are given in the Supporting Information.

Docking vs QSAR. Superimposition of the CoMFA coefficient contour maps (Figure 1) on the ligand (**53**) in the active site of COX-2 is shown in Figure 8. The necessity and usefulness of such comparisons toward a unified pharmacophore model have been discussed by several authors.[34,41−43] However, it is pertinent to emphasize here that combining docking and QSAR data allows for (i) a meaningful correlation between ligand−receptor binding and biological activity, (ii) extrapolation of the SAR beyond the limiting data points, and (iii)

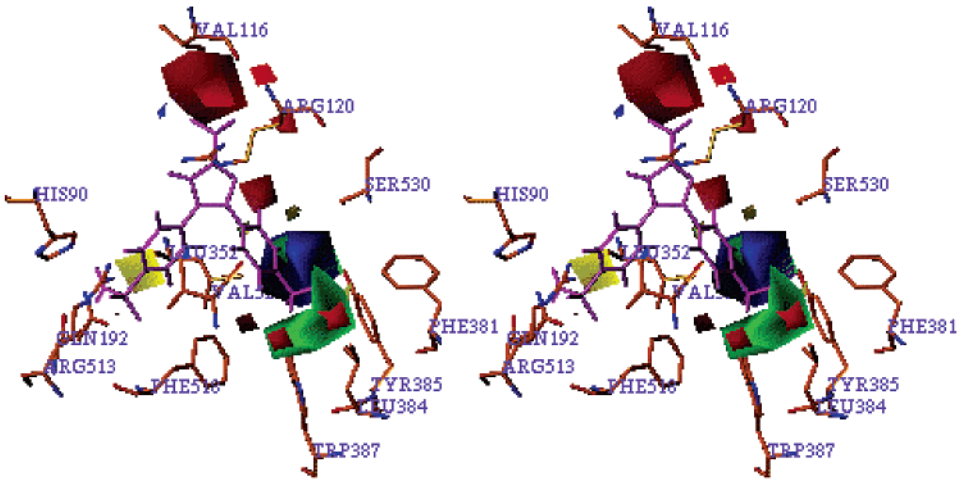

Figure 8. Stereoview of CoMFA steric and electrostatic contour plots (Figure 1) superimposed within the active site of molecule **53**−COX-2 complex.

mutual validation of the two methods and the results obtained in each case.

The red contour above the $-CF_3$ group on ring B suggests that electronegative substituents would enhance the activity—this can be correlated with the presence of the guanidyl group of Arg120 that can form a salt bridge type of strong electrostatic interaction. Similarly, the blue contour near the Cl substituent on ring A merely suggests that the best group for that position should be a less electronegative substituent. In any case, it has no complementary residue in that region. Interestingly, the prominent green contour near the 4-methyl substituent of ring A falls in a hydrophobic pocket consisting of residues Trp387, Tyr385, Leu384, and Phe381. This concurs well with the fact that increasing the bulk would increase the activity. The viability of the QSAR approach is revealed by the fact that the most active molecule, **53**, and the least active molecule, **101**, bind in different orientations. In summary, the correlation of the QSAR data and the docking results mutually validate the intermediacy of a binding step in overall drug action.

Conclusions

CoMFA and CoMSIA analyses of 114 substituted 1,2-diarylimidazoles produced good models with high predictive abilities. The CoMSIA models have slightly higher predictive abilities than the CoMFA. The CoMSIA 2 model with predictive $r^2_{\text{test set}}$ as 0.855 is highly reliable to predict the activities of newly designed molecules. Subsequently, all of the ligands were docked into the active sites of COX-1 and COX-2. The correlation between the docking scores and the activities is very good. A comparison of the 3D QSAR PLS coefficient contour maps with the structural and functional makeup of the binding site also showed good correlation between the two analyses. The docking studies gave good insights into the COX-2−ligand interactions. This information is very crucial in the design and development of COX-2 selective inhibitors as antiinflammatory agents with reduced side effects.

Supporting Information Available: Structures, tables of $-\log(IC_{50})$ values, Van der Waals and electrostatic interaction energies, and sequence similarities. This material is available free of charge via the Internet at http://pubs.acs.org.

Note Added after ASAP Posting

This manuscript was released ASAP on 9/20/2002 without a Supporting Information paragraph. The correct version was posted on 10/17/2002.

References

(1) Mantri, P.; Witiak, D. Inhibitors of COX and 5-lipoxygenase. *Curr. Med. Chem.* **1994**, *1*, 328−355.
(2) Vane, J. R.; Botting, R. Mechanism of action of antiinflammatory drugs. *Scand. J. Rheumatol. Suppl.* **1996**, *102*, 9−21.
(3) Smith, W. L.; Borgeat, P.; Fitzpatrick, F. A. The eicosanoids: COX, lipoxygenase, and epoxygenase pathways. In *Biochemistry of Lipids, Lipoproteins and Membranes*; Vance, D. E., Vance, J., Eds.; Elsevier: New York, 1991; pp 297−325.
(4) Xie, W.; Chipman, J.; Robertson, D. L.; Erikson, R. L.; Simmons, D. L. Expression of a mitogen-responsive gene encoding prostaglandin synthase is regulated by mRNA splicing. *Proc. Natl. Acad. Sci. U.S.A.* **1991**, *88*, 2692−2696.
(5) Vane, J. R.; Botting, R. M. Antiinflammatory drugs and their mechanism of action. *Inflammation Res.* **1998**, *47*, S78−S87.
(6) Katori, M.; Majima, M.; Harada, Y. Possible background mechanisms of the effectiveness of COX-2 inhibitors in the treatment of rheumatoid arthritis. *Inflammation Res.* **1998**, *47*, S107−S111.
(7) DeWitt, D. L. Cox-2-selective inhibitors: the new super aspirins. *Mol. Pharmacol.* **1999**, *4*, 625−631.
(8) Marnett, L. J.; Kagutkar, A. S. Design of selective inhibitors of COX-2 as nonulcerogenic antiinflammatory agents. *Curr. Opin. Chem. Biol.* **1998**, *2*, 482−490.
(9) Hawkey, C. J. COX 2 Inhibitors. *Lancet* **1999**, *353*, 307−314.
(10) Vane, J. R.; Botting, R. M. *Clinical Significance and Potential of Selective COX-2 Inhibitors*; William Harvey Press: London, 1998.
(11) Needleman, P.; Isackson, P. C. Selective inhibition of COX 2. *Sci. Med.* **1998**, *5*, 26−35.
(12) Li, S. H.; Black, W. C.; Chan, C. C.; Ford-Hutchinson, A. W.; Gauthier, J. Y.; Gordon, R.; et al. COX-2 Inhibitors. Synthesis and Pharmacological Activities of 5-Methanesulfonamido-1-indanone Derivatives. *J. Med. Chem.* **1995**, *38*, 4897−4895.
(13) Reitz, D. B.; Li, J. J.; Norton, M. B.; Reinhard, E. J.; Collins, J. T.; Anderson, G. D.; et al. Selective COX Inhibitors: Novel 1,2-Diarylcyclopentenes Are Potent and Orally Active COX-2 Inhibitors. *J. Med. Chem.* **1994**, *37*, 3878−3881.
(14) Schuligoi, R.; Amann, R.; Prenn, C.; Peskar, B. A. Effects of the COX-2 inhibitor NS-398 on thromboxane and leukotriene synthesis in rat peritoneal cells. *Inflammation Res.* **1998**, *47*, 227−230.
(15) Freisen, R. W.; Dubé, D.; Fortin, R.; Frenette, R.; Prescott, S.; Cromlish, W. A.; et al. Novel 1,2-diarylcyclobutenes: Selective and Orally active COX-2 Inhibitors. *Bioorg. Med. Chem. Lett.* **1996**, *6*, 2677−2682.
(16) Silvestre, J.; Lesson, P. A.; Castañer, J. Antiinflammatory COX-2 Inhibitors. *Drugs Future* **1998**, *23*, 598−601.

(17) Penning, T. D.; Talley, J. T.; Bertenshaw, S. R.; Carter, J. S.; Collins, P. W.; Docter, S.; Graneto, M. J.; Lee, L. F.; Malecha, J. W.; Miyashiro, J. M.; Rogers, R. S.; Rogier, D. J.; Yu, S. S.; Anderson, G. D.; Burton, E. G.; Cogburn, J. N.; Gregory, S. A.; Koboldt, C. M.; Perkins, W. E.; Seibert, K.; Veenhuizen, A. W.; Zhang, Y. Y.; Isakson, P. C. Synthesis and Biological Evaluation of the 1,5-Diarylpyrazole Class of COX-2 Inhibitors: Identification of 4-[5-(4-Methylphenyl-3-(trifluoromethyl-1*H*-pyrazol-1-yl]-benzenesulfonamide (SC-58635, Celecoxib). *J. Med. Chem.* **1997**, *40*, 1347−1365.

(18) Prasit, P.; Wang, Z.; Briedeau, C.; Chan, C.-C.; Charlson, S.; Cromlish, W.; Ethier, D.; Evans, J.; Falgueyret, J.-P.; Ford-Hutchinson, A. W.; Gauthier, J. Y.; Gordon, R.; Guay, J.; Gresser, M.; Kargman, S.; Kennedy, B.; Leblance, Y.; Leger, S.; Mancini, J.; O'Neill, G. P.; Ouelett, M.; Percival, M. D.; Perrier, H.; Riendeau, D.; Roger, I.; Tagari, P.; Therien, M.; Vickers, P.; Wong, E.; Xu, L.-J.; Young, R. N.; Zamboni, R.; Boyece, S.; Rupniak, N.; Forrest, M.; Visco, D.; Patrick, D. The discovery of rofecoxib, [MK 966, Vioxx, 4-(4′-methylsulfonylphenyl-3-phenyl-2(5H-furanone], an orally active COX-2 inhibitor. *Bioorg. Med. Chem. Lett.* **1999**, *9*, 1773−1778.

(19) Simon, L. S.; Lanza, F. L.; Lipsky, P.; Hubbard, R. C.; Talwalker, S.; Schwartz, B. D.; Isackson, P. C.; Geis, G. S. Preliminary study of the safety and efficacy of SC-58635, a novel COX 2 inhibitor: efficacy and safety in two placebo-controlled trials in osteoarthritis and rheumatoid arthritis, and studies of gastrointestinal and platelet effects. *Arthritis Rheum.* **1998**, *41*, 1591−1602.

(20) Lloyd, A. W. Monitor: molecules and profiles. *Drug Discovery Today* **2000**, *5*, 121−123.

(21) Sawdy, R.; Slater, D.; Fisk, N.; Edmonds, D. K.; Bennet, P. Use of a cyclo-oxygenase type-2-selective nonsteroidal antiinflammatory agent to prevent preterm delivery. *Lancet* **1997**, *350*, 265−266.

(22) Kutchera, W.; Jones, D. A.; Matsunami, N.; Groden, J.; Mclntyre, T. M.; Zimmerman, G. A.; White, R. L.; Prescott, S. M. Prostaglandin H synthase 2 is expressed abnormally in human colon cancer: evidence for a transcriptional effect. *Proc. Natl. Acad. Sci. U.S.A.* **1996**, *93*, 4816−4820.

(23) Stewart, W. F.; Kawas, C.; Corrada, M.; Metter, E. J. Risk of Alzheimer's disease and duration of NSAID use. *Neurology* **1997**, *48*, 626−632.

(24) Li, C. S.; Black, W. C.; Brideau, C.; Chan, C. C.; Charleson, S.; Cromlish, W. A.; Claveau, D.; Gauthier, J. Y.; Gordon, R.; Greig, G.; Grimm, E.; Guay, J.; Lau, C. K.; Riendeau, D.; Therein, M.; Visco, D. M.; Wong, E.; Xu, L.; Prasit, P. A New Structural Variation on the Methanesulfonylphenyl Class of Selective COX-2 Inhibitors. *Bioorg. Med. Chem. Lett.* **1999**, *22*, 3181−3186.

(25) Dube, D.; Brideau, C.; Deschenes, D.; Fortin, R.; Friesen, R. W.; Gordon, R.; Girard, Y.; Riendeau, D.; Savoie, C.; Chan, C. C. 2-Heterosubstituted-3-(4-methylsulfonylphenyl-5-trifluoromethyl pyridines as selective and orally active COX-2 inhibitors. *Bioorg. Med. Chem. Lett.* **1999**, *12*, 1715−1720.

(26) Lazer, E. S.; Sorcek, R.; Cywin, C. L.; Thome, D.; Possanza, G. J.; Graham, A. G.; Churchill, L. Antiinflammatory 2-benzyl-4-sulfonyl-4H-isoquinoline-1,3-diones: novel inhibitors of COX-2. *Bioorg. Med. Chem. Lett.* **1998**, *10*, 1181−1186.

(27) Bayly, C. I.; Black, W. C.; Leger, S.; Ouimet, N.; Ouellet, M.; Percival, M. D. Structure-based design of COX-2 selectivity into flurbiprofen. *Bioorg. Med. Chem. Lett.* **1999**, *3*, 307−312.

(28) Khanna, I. K.; Weier, R. M.; Yu, Y.; Xu, X. D.; Koszyk, F. J.; Collins, P. W.; Koboldt, C. M.; Veenhuizen, A. W.; Perkins, W. E.; Casler, J. J.; Masferrer, J. L.; Zhang, Y. Y. 2-Diarylimidazoles as Potent, COX-2 Selective, and Orally Active Antiinflammatory Agents. *J. Med. Chem.* **1997**, *40*, 1634−1647.

(29) Khanna, I. K.; Yu, Y.; Huff, R. M.; Weier, R. M.; Xu, X.; Koszyk, F. J.; Collins, P. W.; Cogburn, J. N.; Isakson, P. C.; Koboldt, C. M.; Masferrer, J. L.; Perkins, W. E.; Seibert, K.; Veenhuizen, A. W.; Yuan, J.; Yang, D. C.; Zhang, Y. Y. Selective COX-2 Inhibitors: Heteroaryl Modified 1,2-Diarylimidazoles Are Potent, Orally Active Antiinflammatory Agents. *J. Med. Chem.* **2000**, *43*, 3168−3185.

(30) Desiraju, G. R.; Gopalakrishnan, B.; Jetti, R. K. R.; Raveendra, D.; Sarma, J. A. R. P.; Subramanya, H. S. Three-Dimensional Quantitative Structural Activity Relationship (3D-QSAR) Studies of Some 1,5-Diarylpyrazoles: Analogue Based Design of Selective COX-2 Inhibitors. *Molecules* **2000**, *5*, 945−955.

(31) Desiraju, G. R.; Sarma, J. A. R. P.; Raveendra, D.; Gopalakrishnan, B.; Thilagavathi, R.; Sobhia, M. E.; Subramanya, H. S. Computer-aided design of selective COX-2 inhibitors: comparative molecular field analysis and docking studies of some 3,4-diaryloxazolone derivatives. *J. Phys. Org. Chem.* **2001**, *4*, 481−487.

(32) *SYBYL 6.6 Molecular Modelling Software*; Tripos Associates Inc.: 1699 South Hanley Road, St. Louis, MO 63144.

(33) *INSIGHT 97 Molecular Modelling Program Package*; Molecular Simulations (Accelrys) Inc.: San Diego, CA, 1997.

(34) Gierse, J. K.; Hauser, S. D.; Creely, D. P.; Koboldt, C.; Rangwala, S. H.; Isakson, P. C.; Seibert, K. Expression and Selective Inhibition of the Consititutive and Inducible Forms of Human Cyclooxygenase. *Biochem. J.* **1995**, *305*, 479−484.

(35) (a) Clark, M.; Cramer, R. D., III; Jones, D. M.; Patterson, D. E.; Simeroth, P. E. Comparative molecular field analysis (CoMFA). 2. Toward its use with 3D-structural databases. *Tetrahedron Comput. Methodol.* **1990**, *3*, 47−59. (b) Klebe, G.; Abraham, U.; Mietzner, T. Molecular similarity indices in a comparative analysis (CoMSIA) of drug molecules to correlate and predict their biological activity. *J. Med. Chem.* **1994**, *37*, 4130−4136.

(36) Kurumbail, R. G.; Stevens, A. M.; Gierse, J. K.; McDonald, J. J.; Stegeman, R. A.; Pak, J. Y.; Gildehaus, D.; Miyashiro, J. M.; Penning, T. D.; Seibert, K.; Isakson, P. C.; Stallings, W. C. Structural basis for selective inhibition of COX-2 by antiinflammatory agents. *Nature* **1996**, *384*, 644−648.

(37) Abola, E. E.; Berstein, F. C.; Bryant, S. H.; Koetzle, T. F.; Weng, J. In *Protein Data Bank, in Crystallographic Databases*—*Information Content, Software Systems, Scientific Applications*; Allen, F. H., Berjerhoff, G., Sievers, R., Eds.; Data Commission of the International Union of Crystallography: Bonn, 1987; p 171.

(38) Loll, P. J.; Picot, D.; Ekabo, O.; Garavito, R. M. Synthesis and use of iodinated nonsteroidal antiinflammatory drug analogues as crystallographic probes of the prostaglandin H2 synthase COX active site. *Biochemistry* **1996**, *35*, 7330−7340.

(39) Habeeb, A. G.; Rao, P. N. P.; Knaus, E. E. Design and Synthesis of Celecoxib and Rofecoxib Analogues as Selective Cyclooxygenase-2 (COX-2) Inhibitors: Replacement of Sulfonamide and Methylsulfonyl Pharmacophores by an Azido Bioisostere. *J. Med. Chem.* **2001**, *44*, 3039−3042.

(40) Llorens, O.; Perez, J. J.; Palomer, A.; Mauleon, D. Structural basis of the dynamic mechanism of ligand binding to COX. *Bioorg. Med. Chem. Lett.* **1999**, *9*, 2779−2784.

(41) Price, M. L. P.; Jorgensen, W. L. Analysis of Binding Affinities for Celecoxib Analogues with COX-1 and COX-2 from Combined Docking and Monte Carlo Simulations and Insight into the COX-2/COX-1 Selectivity. *J. Am. Chem. Soc.* **2000**, *122*, 9455−9466.

(42) Chavatte, P.; Yous, S.; Marot, C.; Baurin, N.; Lesieur, D. Three-Dimensional Quantitative Structure−Activity Relationships of Cyclo-oxygenase-2 (COX-2 Inhibitors: A Comparative Molecular Field Analysis. *J. Med. Chem.* **2001**, *44*, 3223−3230.

(43) Vieth, M.; Cummins, D. J. DoMCoSAR: a novel approach for establishing the docking mode that is consistent with the structure−activity relationship. Application to HIV-1 protease inhibitors and VEGF receptor tyrosine kinase inhibitors. *J. Med. Chem.* **2000**, *43*, 3020−3032.

JM020198T